

Beta-gamma burst stimulations of the inferior olive induce high-frequency oscillations in the deep cerebellar nuclei

Julian Cheron^{1,2}  and Guy Cheron^{1,2}

¹Laboratory of Electrophysiology, Université de Mons, Mons, Belgium

²Laboratory of Neurophysiology and Movement Biomechanics, Neuroscience Institute, Université Libre de Bruxelles, Route de Lennik 808, Brussels 1070, Belgium

Keywords: 350 Hz, awake mouse, cerebellum, deep cerebellar nucleus, high-frequency oscillations, inferior olive electrical stimulation

Abstract

The cerebellum displays various sorts of rhythmic activities covering both low- and high-frequency oscillations. These cerebellar high-frequency oscillations were observed in the cerebellar cortex. Here, we hypothesised that not only is the cerebellar cortex a generator of high-frequency oscillations but also that the deep cerebellar nuclei may also play a similar role. Thus, we analysed local field potentials and single-unit activities in the deep cerebellar nuclei before, during and after electric stimulation in the inferior olive of awake mice. A high-frequency oscillation of 350 Hz triggered by the stimulation of the inferior olive, within the beta-gamma range, was observed in the deep cerebellar nuclei. The amplitude and frequency of the oscillation were independent of the frequency of stimulation. This oscillation emerged during the period of stimulation and persisted after the end of the stimulation. The oscillation coincided with the inhibition of deep cerebellar neurons. As the inhibition of the deep cerebellar nuclei is related to inhibitory inputs from Purkinje cells, we speculate that the oscillation represents the unmasking of the synchronous activation of another subtype of deep cerebellar neuronal subtype, devoid of GABA receptors and under the direct control of the climbing fibres from the inferior olive. Still, the mechanism sustaining this oscillation remains to be deciphered. Our study sheds new light on the role of the olivo-cerebellar loop as the final output control of the intercerebellar circuitry.

Introduction

The cerebellum integrates massive sensory inputs from many regions of the brain and spinal cord. This information is used by the cerebellum to coordinate ongoing movements and to coordinate motor learning (Raymond *et al.*, 1996). The cerebellum predicts and controls behavioural outputs through spike trains of information at the millisecond resolution (Heck *et al.*, 2013; Chaisanguanthum *et al.*, 2014) or even over prolonged time windows (Heck *et al.*, 2013; Chaisanguanthum *et al.*, 2014; Popa *et al.*, 2017). The implication of this cerebellar performance in the control and prediction of behaviour has been recognised outside of the sensorimotor field, entering all domains of cognition (Sokolov *et al.*, 2017).

It is well established that, like in other brain areas, neurons in the cerebellum communicate by varying their firing rate but also by discharging at different rhythms (Molinari *et al.*, 2007). The ability to discharge at different rhythms allows them to carry additional

information in a more efficient fashion than the average firing rate as it takes the exact spike timing into account (Jirenhed *et al.*, 2017). The cerebellum displays various sorts of rhythmic activities covering both low-frequency (Courtemanche *et al.*, 2002, 2013; Courtemanche & Lamarre, 2005; D'Angelo *et al.*, 2009; Dugué *et al.*, 2009; Robinson *et al.*, 2017) and high-frequency oscillations (HFO) (Cheron *et al.*, 2004, 2014; Servais *et al.*, 2005; de Solages *et al.*, 2008).

One of the major features of this part of the brain is represented by the closed-loop circuit formed by (i) the Purkinje cells (PC) of the cerebellar cortex, (ii) the deep cerebellar nuclei (DCN) and (iii) the inferior olive (IO) (Hendelman & Marshall, 1980). Each of these neuronal populations is able to fire rhythmically independently from the respective synaptic inputs (Raman *et al.*, 2000; Swensen & Bean, 2003; Masoli *et al.*, 2015; Buchin *et al.*, 2016). Specifically, the IO is characterised by subthreshold oscillations (5–10 Hz) sustained by electrical coupling (Llinas *et al.*, 1974; Long *et al.*, 2002; Leznik & Llinás, 2005).

Axons from the PC produce a strong inhibitory input for different types of DCN neurons (Uusisaari *et al.*, 2007; Uusisaari & Knöpfel, 2008) (Fig. 1). Among these, the GABAergic (GAD67-positive, GAD+IO) neurons are crucial for closing the functional loop between the cerebellar cortex, the DCN and the IO (Ruigrok & Teune, 2014) and control the IO subthreshold oscillations (Lefler

Correspondence: J. Cheron, ²Laboratory of Neurophysiology and Movement Biomechanics, as above. E-mail: jcheron@ulb.ac.be

Received 6 August 2017, revised 12 February 2018, accepted 13 February 2018

Edited by Heleen Slagter. Reviewed by Richard Courtemanche, Concordia University, Canada; and Christian Hansel, University of Chicago, USA

All peer review communications can be found with the online version of the article.

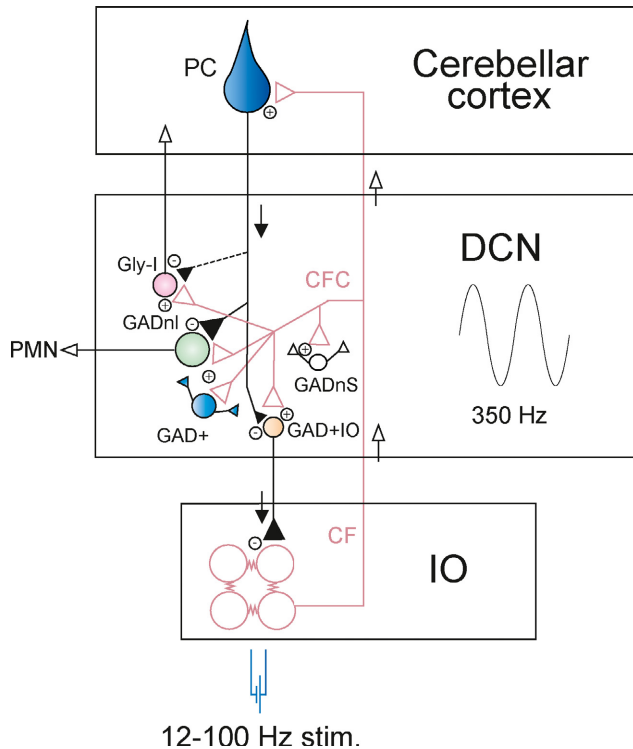


FIG. 1. Scheme of the olivo-cerebellar loop. Schematic drawing of the main pathways and different neuronal units inside the DCN, which may hypothetically participate in the emergence of the 350 Hz oscillation when the inferior olive (IO) is electrically stimulated with a stimulation train ranging from 12 to 100 Hz. The climbing fibres (CF) and their collaterals (CFC) are represented in red. For simplicity, only the Purkinje cell (PC) and its inhibitory projections to the DCN are illustrated in the cerebellar cortex. The neuronal types described in the DCN are based on the definition used by Uusisaari & Knöpfel (2011). Based on GAD67 and GlyT2 promoter activity, these authors have identified four types of neurons in the mouse lateral DCN – namely, (A) the large non-GABAergic (GADnI) neurons mediating nuclear output to premotor nuclei (PMN), (B) the small neurons (GADnS) presenting local synaptic terminations, (C) the nonspontaneously active glycinergic neurons (Gly-I) mediating nuclear output to the cerebellar cortex and (D) the GABAergic neurons with local connections (GAD+) and a special subtype of this neuron category projecting to the IO (GAD+IO). The synapses schematised in black and white represent inhibitory and excitatory elements, respectively.

et al., 2014; Mathy *et al.*, 2014). The output of the IO is formed by climbing fibres (CF) that subsequently activate the DCN (by CF collaterals) and the cerebellar cortex (by CF terminals) (Fig. 1).

The activation of the CF produces a distinctive electrophysiological fingerprint on the PC called complex spike (CS) (Eccles *et al.*, 1966; Llinás & Sugimori, 1980a,b). This IO input to the PC is an important cue for the function of the cerebellar cortex, conveying both timing information and triggering synaptic plasticity (Gilbert & Thach, 1977; Hansel *et al.*, 2001; Ito, 2001). It is now well established that the olivo-cerebellar system is involved in the control of ongoing motor commands (Welsh *et al.*, 1995; Llinás, 2011, 2013; Schweighofer *et al.*, 2013; Chen *et al.*, 2016; Streng *et al.*, 2017; White & Sillitoe, 2017).

At the circuitry level, due to the massive convergence of PC axons towards the DCN neurons [roughly 200,000 PC (Woodruff-Pak, 2006) towards approximately 30,000 DCN neurons (Sultan *et al.*, 2002)], the oscillatory state of the cerebellar cortex can spread strongly towards DCN neurons. From there, the oscillation can be transmitted to the IO, and, sequentially, the signal output of the CF

collaterals controls the GABAergic neurons of the DCN (De Zeeuw *et al.*, 1997). Indeed, the rhythmic imprint of the IO influences not only the cerebellar cortex but also the DCN complex (directly by the excitatory CF collaterals and indirectly by the inhibitory PC axons). Still, the impact of IO's activation on the DCN is not well characterised but might be one of the multiple ways by which the olivo-cerebellar activity exerts strong influence on the cerebellar function.

This reasoning can be sustained by two observations from our group: (i) knockout mice for calcium-binding proteins presented a CS phase-locked to a 160 Hz local field potential (LFP) oscillation generated by a set of synchronous PCs (Cheron *et al.*, 2004; Servais *et al.*, 2005), and (ii) knockout mice for BK channels presented a CS phase-locked to a beta oscillation (Cheron *et al.*, 2009). These observations indicate that the different types of cerebellar oscillations from beta to high-frequency output generated in the PCs are transmitted via the DCN to the IO and not restricted only to the cerebellar cortex. More recently, the HFO were also described in wild-type animals, though with a weaker oscillation power (de Solages *et al.*, 2008; Groth & Sahin, 2015).

Here, we address the question of how the DCN responds to rhythmic activity and whether it can be *per se* a generator of HFO. For this purpose, we analysed the LFP and the single-unit activities in the DCN before, during and after the IO stimulations in awake mice. We showed for the first time the appearance of a 350 Hz oscillation in the DCN triggered by IO stimulation.

Materials and methods

Mice

C57Bl6 mice ($n = 5$), 5–8 months of age, obtained from an authorised supplier (Charles River Laboratories, Wilmington, MA, USA), were used as experimental animals. All mice were housed up to four mice per cage in an animal room at 22 °C under a 12-h light/dark cycle (light on at 7 a.m.) with *ad libitum* access to food and water. All animal procedures were approved by the University of Mons Ethics Committee and conducted in conformity with the European Union directive 2010/63/EU. During the 24-h postoperative period, warmth and free access to high-energy liquid were provided. Every effort was made to minimise the number of animals and their discomfort.

Surgical preparation

The mice were anaesthetised with xylido-dihydrothiazin (10 mg/kg, Rompun®; Bayer, Leverkusen, Germany) and ketamine (100 mg/kg, Ketalar®; Pfizer, New York, NY, USA). The animals were administered an additional dose of xylido-dihydrothiazin (3 mg/kg) and ketamine (30 mg/kg) when agitation or marked increases in respiration or heart rate during the procedure were noted. In addition, local anaesthesia [0.5 ml of 20 mg/ml lidocaine and adrenaline (1 : 80 000, Xylocaine®; Astra Zeneca, Cambridge, UK)] was administered subcutaneously during the soft tissue removal. During surgery, two small bolts were cemented perpendicular to the skull to immobilise the head during the recording sessions, and a silver reference electrode was placed on the surface of the parietal cortex. To allow access to the DCN, the surface of the cerebellum was exposed, and an acrylic recording chamber was constructed around a posterior craniotomy (2 × 2 mm) and covered with a thin layer of bone wax (Ethicon®; Johnson & Johnson).

In addition, bipolar silver stimulating electrodes were vertically implanted in the IO: 7.2 mm posterior, 0.25 mm lateral and 4.5 mm deep, from the Bregma, following the method developed by Gruart *et al.* (1994). Electrodes were aimed at the centre of the mentioned structures and inserted contralaterally from the site of DCN recording following the stereotaxic coordinates from the atlas of Paxinos and Franklin (1997).

Electrical stimulation of the inferior olive

The IO was electrically stimulated at different frequencies (1, 12, 30, 50 and 100 Hz) with a total duration of 1 s, when a single DCN neuron was stably recorded. The electrical stimulation unit consisted of an initial single negative square pulse of 0.2 ms followed by a positive square pulse of 0.1 ms in duration and of 2 mA current intensity, delivered by an isolation unit (IsoFlex, AMPI, Israel) connected to an analogue pulse generator (Master 8, AMPI, Israel). The amplitude of the current was adjusted to avoid overt movements and animal discomfort.

Histological identification of the recording and stimulating sites

At the end of the experiment, electrolytic marks were placed in the DCN with quartz–platinum/tungsten microelectrodes (1 mA for 10 s). Then, the animals were deeply anaesthetised with sodium pentobarbital (50 mg/kg, i.p.) and transcardially perfused with saline and phosphate-buffered formalin. To control the correct positioning of the stimulating and recording electrodes, serial 50- μ m-thick sections of the brainstem and cerebellum mounted on glass slides and stained with Cresyl Violet were produced. Only the recordings performed specifically in the interpositus nucleus (DCN nucleus) and the stimulating site located in the IO were used in our study.

Single-unit and multiple-unit recordings in alert mice

Twenty-four hours after anaesthesia, the alert mice were restrained for the recording session. The dura mater was removed over the cerebellum to expose the tissue in the recording chamber. Using stereotaxic coordinates and the shape of recordings, the correct position of the electrodes was achieved. To avoid unnecessary stress for the animals and movement artefacts, the recording sessions were performed in a quiet room, when the animals were awake and calm. The alertness level was controlled by whisker activity during the recording session. We used quartz–platinum/tungsten microelectrodes (1.2–3 M Ω) in a seven-channel Eckhorn microdrive (Thomas Recordings©, Giessen, Germany). All measures of impedance were made with a 1 kHz sinusoidal current and checked throughout the recording session. In this study, the explorations were made with a microelectrode (outer and shaft diameters of 80 and 25 μ m, respectively). The microelectrode was mounted onto a stretched elastic rubber tube to enable proper positioning via DC micromotors (resolution of 0.27 μ m).

Data analysis and statistical methods

Neural activity signal recordings were filtered at 100 Hz high pass and 10 kHz low pass. LFP and unitary electrical activities were stored digitally on a computer after conversion with an analog–digital converter (Power 1401; CED©, Cambridge, UK). The recorded data were digitised continuously at 20 kHz. Offline analysis and illustrations were performed with Spike 2 CED software (CED©).

Fast Fourier transform (FFT) analyses were performed during the different intervals between every successive pulse along the trains of stimulation, before the stimulations and during the inhibition periods of the DCN neuron firing (930.7 ± 412.6 ms). Hanning windows size ranged from 512 points (in 256 bins, resolution of 39.06 Hz) to 2048 points (in 1024 bins, resolution of 9.7 Hz) depending on the available time periods.

Parametric data, provided by the Kolmogorov–Smirnov test, were analysed using a Student's *t*-test, one-way and two-way ANOVA tests and Bonferroni's or Dunnett's *post hoc* tests when appropriate. For nonparametric data, the Wilcoxon matched pairs test or the Kruskal–Wallis test was also used for multiple comparisons. Differences were considered significant when $P < 0.05$. The results are expressed as mean \pm standard deviation or standard error of mean when applicable.

Results

350 Hz oscillation in the DCN evoked by IO stimulation

Inferior olive stimulations were applied during the stable recording of 48 DCN neurons. Among these neurons, 15 were not responding to the IO stimulation, while in the 33 remaining neurons, a total of 47 stimulation trains (out of 85), fixed at 12, 30, 50 or 100 Hz in the IO, evoked a high-frequency LFP oscillation peaking at 354.0 ± 60.9 Hz (ranging from 214.0 to 513.0 Hz). The length of each train of stimulation was fixed at 1 s for every applied frequency.

High-frequency oscillations did not occur spontaneously but only when frequencies above 12 Hz were evoked by the stimulation of the IO. When 1 Hz stimulation was applied, no HFO were observed. Only trains of stimuli fixed at 12 Hz or higher frequencies (30, 50, 100 Hz) were able to induce this phenomenon.

IO stimulations induced two simultaneous effects: a well-known inhibition period and an HFO

Figure 2 illustrates the presence of this LFP oscillation at the end of the stimulation train (30 Hz). The firing of DCN neurons was completely inhibited by the stimulation of the IO (Fig. 2A) during a mean inhibition period of 930.7 ± 412.6 ms (ranging from 320.0 to 2004.0 ms) ($n = 47$ stimulations). The HFO (Fig. 2B–C) largely occurred during this inhibition period and progressively ended when the inhibition period of the DCN neurons was finished. In addition, small positive spikes were in some cases present on top of the LFP oscillation (Fig. 2E) and also disappeared after the inhibition period.

Figure 3A highlights the difference between the recording trace in the absence (upper trace) and in the presence of this 350 Hz oscillation (lower trace). The frequency (Fig. 3B) and the power (Fig. 3C) of the HFO did not significantly depend on the stimulation frequency used (12, 30, 50 and 100 Hz), ($F_{3,43} = 2.74$, $P = 0.055$; and $F_{3,43} = 2.58$, $P = 0.0657$, respectively, one-way ANOVA), indicating that this type of oscillation was not related to artificial resonance linked to the stimulation current.

The 350 Hz oscillation emerged progressively during the stimulation

To better understand the nature of this oscillation, we analysed its initiation during the stimulation period (Fig. 4). FFT analyses were performed during the different intervals between every successive pulse along the train of stimulation (# epochs). Figure 4(A–D)

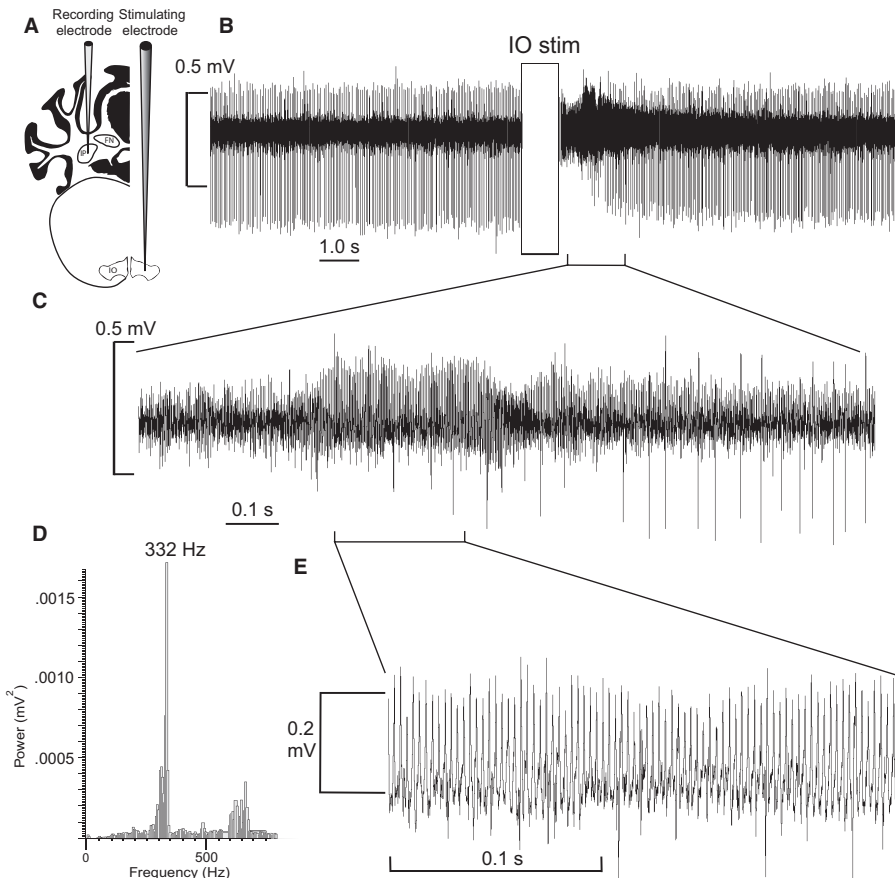


FIG. 2. Emergence of a high-frequency LFP oscillation after a 30 Hz IO stimulation. (A) Scheme of the recording and stimulating electrodes' locations. (B) Typical extracellular recording of a DCN neuron before and after the application of a train of electrical stimuli given at 30 Hz (white rectangle) in the IO. Note the inhibition period during which a high-frequency oscillation occurred. (C) Expanded view of the LFP oscillation. (D) FFT histogram (from 0 to 2,000 Hz with FFT size of 2048 points [Hanning window] and resolution of 9.76 Hz) of the LFP oscillation peaking at 332 Hz. (E) A further magnification of the LFP oscillation demonstrates the presence of a small positive spike at the top of the oscillation. IP: interpositus nucleus, FN: fastigial nucleus, IO: inferior olive.

illustrates an example of the FFT analysis during the 30 Hz stimulation from the stimuli #1 to #30 of the train. We observed a progressive appearance of the 350 Hz oscillation during the stimulation period with some early tentative (e.g. #2 and #5, Fig. 4D) and weakness (e.g. #3, #4, Fig. 4D) before a clear emergence around the middle of the stimulation train (e.g. after #16, Fig. 4C). The histograms shown in Fig. 4C–D are based on the signal illustrated in Fig. 4A–B. We systematically observed the persistence of the oscillation after the end of the stimulation (Fig. 2D). To precisely analyse the beginning of the oscillatory content, we applied four successive trains of stimulation (30 Hz) during the recording of one DCN neuron (the corresponding raw signal during the second stimulation train is illustrated in Fig. 4F). We then compared the mean ($n = 4$) maximal FFT power between 300 and 400 Hz for each of the 29 epochs with the mean ($n = 4$) 300–400 Hz maximal FFT power before the stimulation. Some values along the stimulation were significantly different from the power of the oscillation before the stimulation (Kruskal–Wallis test, multiple comparison, $P = 0.0318$, see Fig. 4E for a more detailed view of the multiple comparison test). FFT values (means of the maximum power between 300 and 400 Hz) showed that the 350 Hz emerged progressively along the train (Fig. 4E). These results demonstrated that this oscillation appears during the stimulation period and is consequently not induced by the arrest of the stimulation train. We might consider that this oscillation is not a posteffect.

Impact of the stimulation trains on the evoked diphasic field

As the single pulse stimulation applied in the IO evoked a diphasic field (negative–positive) (Fig. 5A) of stable amplitude appearing at a mean latency of 3.2 ± 0.5 ms in the DCN after the stimulation, we have analysed the effect of the stimulation train (and its frequency) on the diphasic field. Figure 5A shows an example of a diphasic field potentiation during the 100 Hz stimulation. Trains of stimulation fixed at 50 and 100 Hz induced an immediate potentiation of the field (appearing at the #2 stimulation), reaching, respectively, 226 and 342% of their initial amplitudes (Fig. 5B). These significant increases (two-way ANOVA [interaction factor: $P < 0.0001$, repetition factor: $P < 0.0001$] with Dunnett's multiple comparisons, respectively, $P < 0.001$ and $P < 0.0001$) were maintained during the train. A significant increase is observed for the 30 Hz stimulation after the sixth stimulation (#6) (two-way ANOVA, Dunnett's multiple comparisons test, $P < 0.05$) but was not maintained. No potentiations of the diphasic field were observed during a 12 Hz train of stimulation (Fig. 5B).

Beta-gamma stimulations induced an inhibition-rebound pattern in the DCN

The way DCN neurons fire in response to a single pulse stimulation applied in the IO (at 1 Hz frequency) was analysed on 48 neurons.

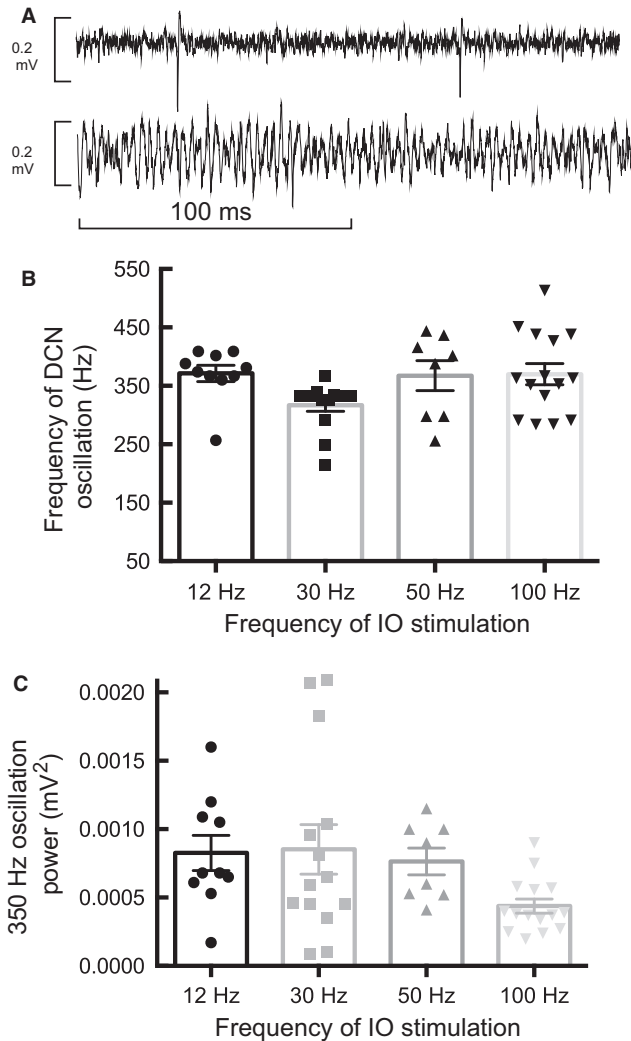


FIG. 3. Effects of the different train frequencies of the IO stimulation. (A) Comparison of recordings in the DCN in the absence (upper trace) and in the presence (lower trace) of the 350 Hz. Note the presence of two DCN neuron spikes. (B) Mean frequencies \pm SEM of the LFP oscillations evoked by four different stimulation trains at the following frequencies: 12 Hz, $n = 10$; 30 Hz, $n = 14$; 50 Hz, $n = 8$; and 100 Hz, $n = 15$ (degrees of freedom for both tests = 43). (C) Mean powers of the LFP oscillation evoked by the same stimulation trains as in A.

The mean firing rate at the baseline was 37.4 ± 18.0 Hz (ranging from 11.0 to 83.0 Hz, $n = 48$). Among these 48 recordings, only 33 were responsive to the IO stimulation. Figure 6A illustrates a representative DCN neuron. The first group of spikes (one to five spikes) was evoked at a latency of 6.1 ± 2.2 ms (ranging from 3.4 to 14 ms and recorded in 33 neurons) (first white triangle, Fig. 6A) followed by a second group at a latency of 19.9 ± 8.7 ms, (recorded in 22 neurons) (second white triangle, Fig. 6A) followed by a longer inhibition at a midlatency of 60.3 ± 17.2 ms (recorded in 29 neurons) (black triangle, Fig. 6A). This inhibition was followed by a rebound at about 100 ms, (recorded in 29 neurons, third white triangle, Fig. 6A).

Inversely, all the other tested frequencies (12, 30, 50 and 100 Hz) of trains of stimulation were followed by a firing rate sequence of inhibition followed by a rebound; no early evoked 'spiking' period was recorded. Figure 6B–C illustrates this effect on one representative DCN neuron after a 30 Hz stimulation. Ten stimulations applied

on the same DCN neuron are pooled together in the Fig. 6C. Before this 30 Hz stimulation, the mean firing rate was 17.25 ± 1.23 Hz and 32.60 ± 20.36 after the inhibition period (rebound) ($n = 10$ stimulations, Wilcoxon matched pairs test, $P = 0.0020$).

Discussion

We demonstrated the emergence of a HFO at 350 Hz in the DCN when trains of electric stimulation were applied to the IO. This oscillation emerged during the train of stimulation and continued after the end of the stimulation. In some cases, positive spikes also emerged on top of the LFP oscillation, suggesting a neuronal origin for this HFO. As the oscillation coincides temporally with the inhibition of DCN neurons that were previously active, we speculate that it represents the unmasking of the synchronous activation of a subtype of DCN neurons under the direct control of the CF collaterals from the IO that are not targeted by the PC.

Other HFO already described

High-frequency oscillations (200–600 Hz, fast ripples) have been described during whisker and thalamic stimulation in the (normal) barrel cortex of rats (Kandel & Buzsáki, 1997; Jones & Barth, 1999; Jones *et al.*, 2000). It is interesting to note that the FFT peak of the HFO evoked by whisker stimulation in awake rats reported previously (Jones & Barth, 1999) coincides perfectly with this newly observed 350 Hz HFO. These cortical HFO could play an important role in the processing of cortical information in the somatosensory cortex (Jones *et al.*, 2000; Barth, 2003). At present, we still do not completely understand the mechanisms underlying these HFO. Interneurons were initially seen as a potential source of this HFO, but the injections of GABA_A antagonists were not able to suppress it (Jones & Barth, 2002), leaving three possible explanations: (i) the contribution of another type of inhibitory interneurons; (ii) the intervention of electrically coupled neurons by axonal gap junctions as reported in the hippocampus (Traub & Bibbig, 2000; Traub *et al.*, 2012), cerebral (Traub *et al.*, 2011; Simon *et al.*, 2014) and cerebellar cortex (Cheron *et al.*, 2004; Traub *et al.*, 2008) (note that gap junctions are present in the DCN [Van Der Giessen *et al.*, 2006;]; and (iii) the presence of more complex mechanisms, including somatic inhibition and dendritic excitation (English *et al.*, 2014). Similar to our present data, these cortical HFO were followed by spike suppression and noticeable after hyperpolarisation. HFO were also identified by FFT analyses of somatosensory evoked potentials in humans (Curio *et al.*, 1994; Waterstraat *et al.*, 2016).

Single stimulation of the IO evoked the classical response of excitation–inhibition and rebound

Although the DCN neurons are heterogeneous (Uusisaari & Knöpfel, 2011), the range and the mean of the baseline firing of the present DCN neurons fitted well with those reported in alert preparation from different species (Thach, 1968; Armstrong & Rawson, 1979; Gruart & Delgado-García, 1994). The present DCN neuron firing recorded in awake mice in response to single pulses applied in the IO stimulation resembles that recorded in anaesthetised rats by Hoebeek *et al.* (2010). The sequence was characterised by an initial excitatory response corresponding to the input of the CF collaterals followed by inhibition and rebound. This early evoked response (3.4 ms) fits well with that reported after optogenetic stimulation *in vitro* (3.3 ms) (Najac & Raman, 2017). Nevertheless, here we observed a stronger excitatory

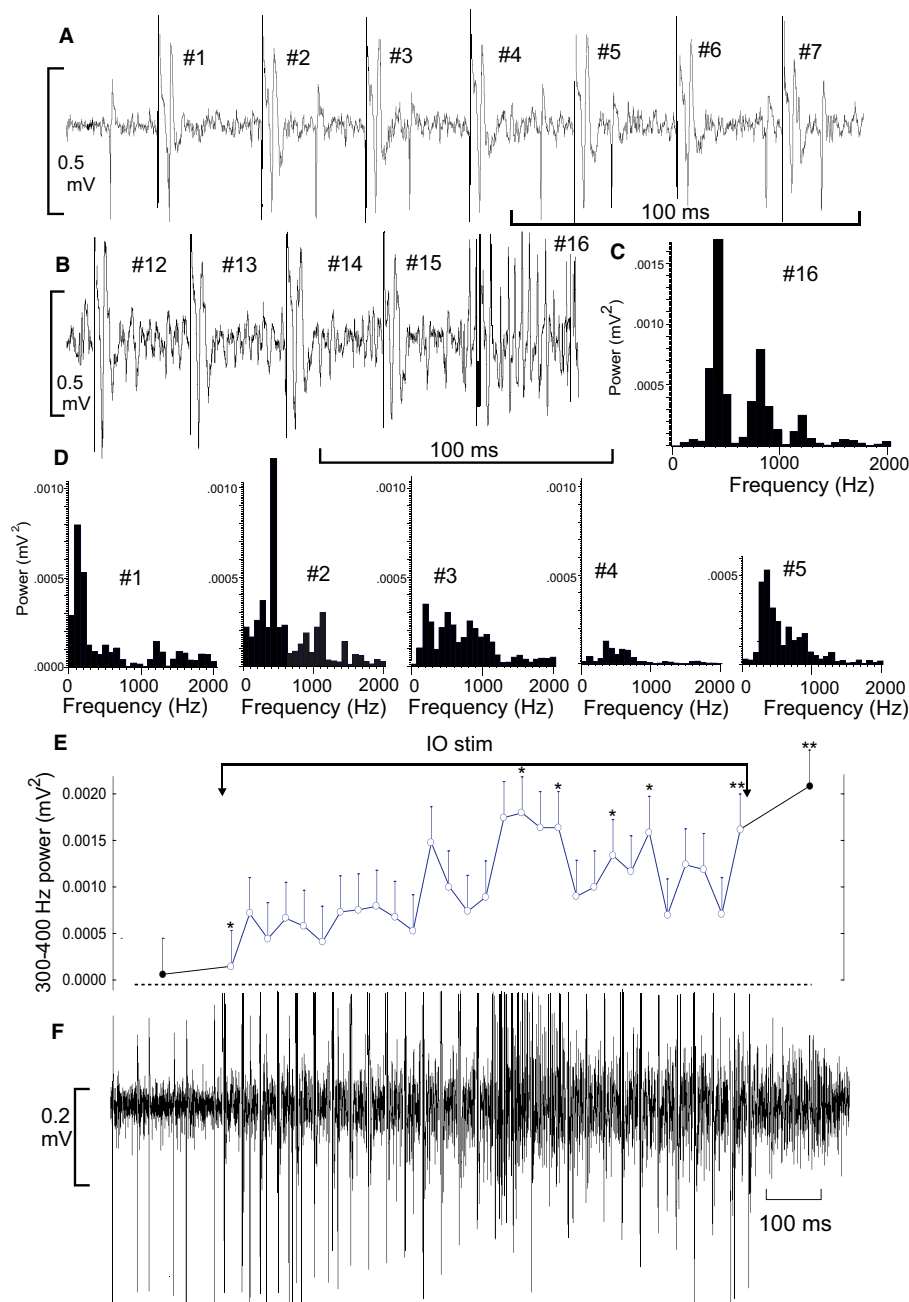


FIG. 4. Emergence of the 350 Hz during the IO stimulation train. (A) Raw traces of a representative DCN neuron during the IO stimulation train at 30 Hz during the first sequence of stimuli (from #1 to #7) showing the DCN neuron spikes, the stimulation artefact and the diphasic field potentials. (B) Idem as in A but for a following period of stimuli (from #12 to #16). (C) The FFT histogram (from 0 to 2.000 Hz with FFT size of 512 points [Hanning window] and resolution of 39.06 Hz) corresponding to interval #16 showing the emergence of the 350 LFP oscillation. (D) Same type of FFT histograms corresponding to the interval #1 to #5. (E) The maximal FFT power between 300 and 400 Hz during the stimulation ($n = 4$ consecutive stimulations on one isolated DCN neuron). Some values along the stimulation were significantly different from the power of the oscillation before the stimulation (Kruskal-Wallis test, multiple comparison, $P = 0.0318$, $*P < 0,05$, $**P < 0,001$). (F) Recording of the same DCN neuron as in E during the IO stimulation train at 30 Hz.

response with two successive excitations before the occurrence of the inhibition and a late rebound. As the same current intensity (about 0.2 mA) was used in the two studies, we think that the difference in intensity could be due to the presence of ketamine in the rat preparation. Considering the crucial role played by the *N*-methyl-D-aspartate (NMDA) receptors in DCN neurons (Pugh & Raman, 2006), their blockade by ketamine (Anis *et al.*, 1983) may explain the weaker excitation induced by the IO stimulation in this latter preparation.

The nature of the diphasic field potential evoked by IO stimulation

It is noteworthy that, similar to the report of Hoebek *et al.* (2010), we never observed the antidromic activation of DCN neurons after IO stimulation. Nevertheless, a diphasic field potential was observed, resembling that reported by Gruart *et al.* (1994). The early negative part of this field is probably a readout of the antidromic stimulation of the DCN neurons projecting to the IO. Indeed, Llinás &

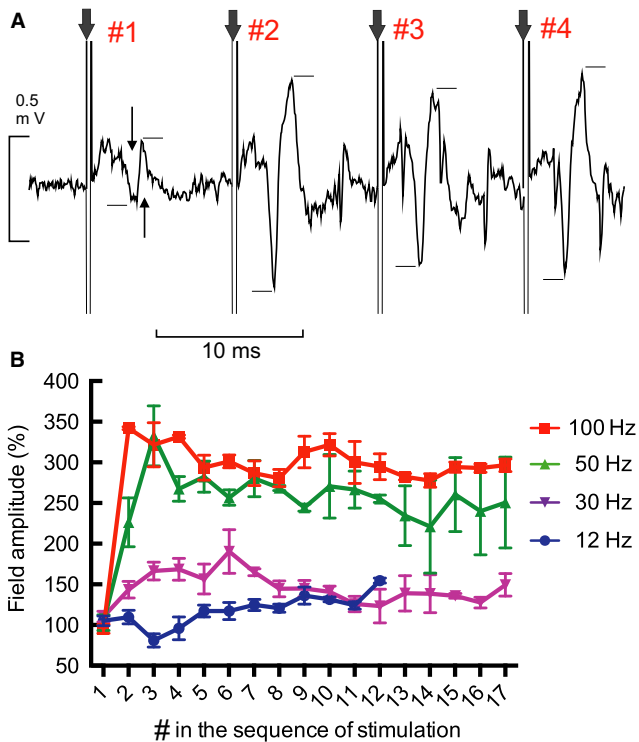


FIG. 5. Potentiation of the diphasic field potentials. (A) Diphasic field potentials evoked by the IO stimulation train and recorded in the DCN. The first four stimulations of a 100 Hz stimulation train are illustrated. Black vertical arrows point to the single IO stimulation artefact. (B) Evolution of the diphasic field amplitude (peak-to-peak) (\pm SEM) from the 1st to the 17th stimuli in the 30, 50 and 100 Hz frequencies of the IO stimulation train and from the 1st to the 12th for the 12 Hz stimulation.

Mühlethaler (1988) and Gruart *et al.* (1994) interpreted the higher negativity of this field potential as a consequence of the synaptic excitation of the DCN neurons by the CF collaterals. The interpretation of the delayed positivity being a form of synaptic inhibition from the PC is not applicable as its latency (4.5 ms) is too short to propagate via the cerebellar cortex.

DCN excitation–inhibition–rebound, the diphasic field potential potentiation and the appearance of the 350 Hz HFO

Although the excitation–inhibition sequence was reported in the present study, when a single stimulus was applied at the IO, the excitation phase was not observed at the end of the application of repeated stimuli (trains of 12–100 Hz). At the end of the train of stimulation, only the inhibition of the ongoing firing of the DCN neurons and the arrival of the 350 Hz oscillation occurred before the resurgence of the DCN firing and the subsequent rebound. The absence of this early spiking phase could be explained by the accumulation of the PC inhibitory effect along the stimulation period. It is probable that the inhibitory input of the synchronised PC overrides the general state of the DCN (Lu *et al.*, 2016), taking into account the prevalence of the PC synapses in the DCN (De Zeeuw & Berrebi, 1995).

The inhibition phase of the DCN firing contrasted with the potentiation of the diphasic field potential. Spatial and temporal synaptic plasticity might explain the huge amplification of this diphasic field potential. The amplification of this diphasic field has been previously reported by Gruart *et al.* (1994) during the repetitive stimulation of the IO and the conditioning stimulation of the pontine

nucleus. The same authors also mentioned that this field might be greatly potentiated by different sensory inputs. As this field potentiation was in the present study followed by the emergence of the 350 Hz oscillation, it might reflect a new multisensory integrating function reinforcing the potential influence of the CF collateral input on the DCN.

Selectivity of the stimulation

In comparison with what could be achieved with chemo- and optogenetic stimulations, we need to consider the possible lack of selectivity of the electrical stimulation. Indeed, the electrical stimulation might have activated neurons other than IO neurons and their CFs. In particular, mossy fibres could be partially involved in the reported DCN firing pattern. However, a strong recruitment of CF and not of mossy fibres was easily achieved probably thanks to the configuration of the IO (packed IO neurons and bundle of CF contrasting with a dispersed organisation of the mossy fibres). The fact that small single pulses (stimulation currents < 0.2 mA) were able to evoke CS at a latency of 10 to 20 ms without any change in the firing of the simple spike of the recorded PC is another argument in favour of a limited influence of mossy fibres' excitation by the IO stimulation.

Physiological relevance of the 350 Hz oscillation

The physiological relevance of the present findings must be questioned considering the electrophysiological approach used for the induction of the 350 Hz oscillation in the DCN. Indeed, it is commonly admitted that the IO output carried by the CF is about 0.4 to 1.5 Hz in resting mode (Cheron *et al.*, 2004; De Gruijl *et al.*, 2014), 3–5 Hz during behavioural learning (Gilbert & Thach, 1977; Márquez-Ruiz & Cheron, 2012) and 9–12 Hz when the IO is actively hyperpolarised (Linás & Yarom, 1986). In contrast, the frequencies of electrical stimulations used in the present study were different from the commonly reported ranges. However, recent evidence tempers the possibility that the present findings would not be physiologically relevant. Indeed, Najac & Raman (2017) demonstrated that a DCN EPSC registered after IO stimulation is formed by multiple wavelets that could be the result of CF axon bursting and multiple CF collaterals. The fact that it is possible to enhance associative short-term plasticity (the synaptically evoked suppression of excitatory PF-PC synapses, see Brenowitz and Regehr, 2005) using a short burst stimulation of CF at 400 Hz (Mathy *et al.*, 2009) could be seen as an argument in favour of a physiological plausibility of the beta-gamma stimulation rate. Moreover, the fact the DCN neuron firing rate increased from a baseline of 56 Hz to 269 Hz after optogenetic stimulation of the IO *in vitro* is in favour of the physiological significance of the 350 Hz oscillation, which can be supported by such increase in the DCN neurons firing rate (Najac & Raman, 2017).

Nevertheless, the duration of the stimulation (1 s) at these high frequencies may be questioned. Indeed, a 1-s neuronal activity at these high frequencies has never been found in a physiological context. This leaves open whether the finding is physiologically relevant.

It should also be mentioned that, even if we stimulated at relatively high frequencies, the IO output might occur at other rate ranges. It is still possible that the stimulations recruit inhibitory cells inside of the IO or inhibitory axonal terminations (e.g. from the DCN) that could temper the output rhythm. The present approach needs to be further confirmed with direct recordings into the IO

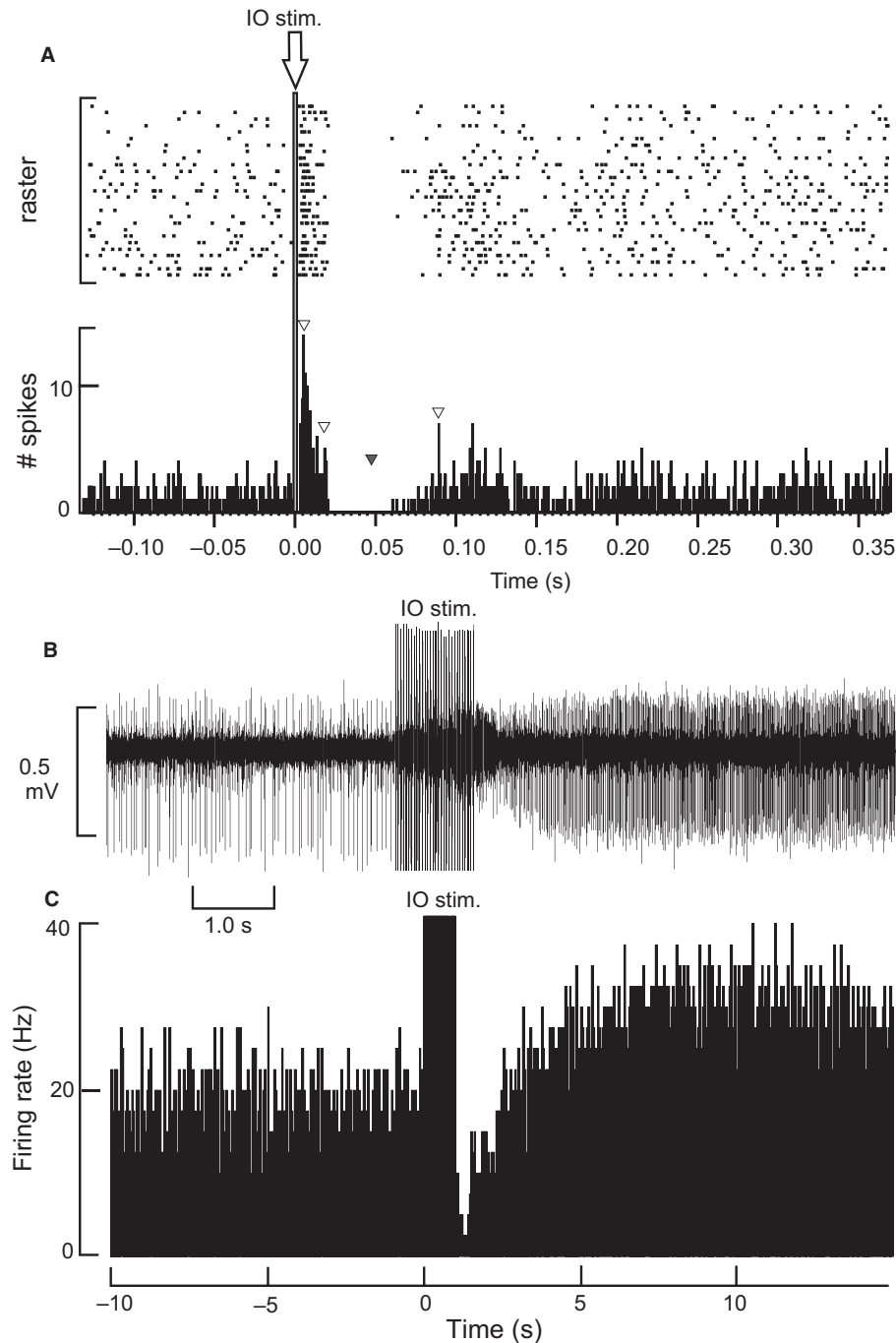


FIG. 6. Firing pattern of DCN neurons evoked by single and train stimulations of the IO. (A) Firing activity of a representative DCN neuron before and after single stimulations (1 Hz) of the IO. Raster (upper part) and firing histogram highlighting early excitatory responses (first white triangle) at approximately 6 ms and 20 ms (second white triangle) followed by an inhibition period (black triangle) centred to approximately 60 ms. (B) Recording of a DCN neuron before and after a train of IO stimulation (30 Hz). Note the presence of firing rate inhibition during the high LFP oscillation followed by a rebound in the firing. (C) Histogram of the mean firing rate of the same DCN neuron as in B before and during trains of stimulation ($n = 10$ 30 Hz stimulations). IO stimulation corresponds to the stimulation artefact.

during beta-gamma stimulation in order to characterise its real effect on the DCN input.

The possible mechanisms of the 350 Hz oscillation

Here, we observed an apparent paradox: two opposite electrophysiological events evoked by the electrical stimulation of the IO at the same time (the inhibition of neuronal firing of the ongoing DCN

firing and the emergence of a 350 Hz HFO). The inhibitory response is currently explained by the PC inhibitory input to the DCN. Thus, elucidating the emergence of the 350 Hz HFO that happened concomitantly with a global inhibition phase is challenging. As it was reported that this synaptic inhibition is equally transmitted to all DCN neurons and that fast DCN oscillation has not yet been spontaneously recorded, the repeated excitation provided by the convergence of the CF collaterals must play a trigger role for the

initiation of the oscillation. The tetanic stimulation of the PC axons is able to produce long-term depression in the DCN neuron (Sastry *et al.*, 1997), which may facilitate the emergence of the 350 Hz oscillation.

Deep cerebellar nucleus interneurons might contribute to the emergence of the 350 Hz. In fact, the repeated excitatory inputs from the CF collaterals could activate the DCN interneuron pool. However, the importance of the interneuronal pool of the DCN seems to be minimal and represent only 15% of the GABAergic innervation in the mouse DCN (Houser *et al.*, 1984; Wassef *et al.*, 1986). The fact that the vast majority of DCN neurons [95% in cats (McCrea *et al.*, 1978)] project outside of the DCN does not preclude the possible participation of these small inhibitory neurons to the 350 Hz oscillation. After all, this 350 Hz oscillation could be supported by a special class of DCN neurons, expressing a rather low level of GABA receptors, and thus less impacted by the inhibition of the PC. DCN glycinergic interneurons seem to express a rather low level of GABA receptors (Husser *et al.*, 2014). These neurons represent 5% of the inhibitory input to principal DCN neurons and produce fast IPSCs, which could be able to support fast LFP oscillation. A local DCN network might be involved and could implicate gap junctions. Conversely, a long loop connecting the IO, the DCN, the PC and the IO or even a shorter DCN–IO–DCN loop cannot be involved considering the time spent in the conduction of the signal around the loop (at least 10 ms for the shorter loop), which is incompatible with the HFO rate of oscillation.

In conclusion, we observed in the present study a new oscillation in the olivo-cerebellar loop, shedding light on a new rhythmic control of the output signal of the cerebellum. The mechanisms underlying the emergence of the 350 Hz oscillation during this particular state of DCN inhibition remain largely undetermined at this stage and should be studied with more sophisticated approaches in awake animal preparations. The first step would be to demonstrate the same observation using intracellular or patch-clamp recordings with optogenetic stimulations in awake animals.

Acknowledgements

We would like to thank T. D'Angelo, E. Pecoraro, M. Dufief, E. Toussaint, E. Hortmanns and M. Petieau for expert technical assistance. We also thank D. Rial (ULB, Brussels) for detailed comments on the manuscript. J.C. is supported by a grant from the Fonds Erasme (ULB) and the Belgian National Fund for Scientific Research (FNRS). This work was funded by the Belgian Federal Science Policy Office, the European Space Agency (AO-2004, 118), the Belgian National Fund for Scientific Research (FNRS), the research funds of the Université Libre de Bruxelles and of the Université de Mons (Belgium) and the Fonds G. Leibn.

Conflict of interest

The authors declare that the research was conducted in the absence of any commercial or financial relationships that may represent a potential conflict of interest.

Data accessibility

The article's supporting data and materials can be accessed at the Laboratory of electrophysiology, Université de Mons, Mons, Belgium.

Author contributions

J.C. performed the experiment, analysed the data, drafted the article and revised the article. G.C. performed the experiment, analysed the data, drafted the article and revised the article.

Abbreviations

CF, climbing fibres; CFC, climbing fibre collaterals; CS, complex spike; DCN, deep cerebellar nuclei; FFT, fast Fourier transform; FN, fastigial nucleus; GABA, gamma-aminobutyric acid; HFO, high-frequency oscillation; IO, inferior olive; IP, interpositus nucleus; LFP, local field potential; NMDA, n-methyl-D-aspartate; PC, Purkinje cell.

References

- Anis, N.A., Berry, S.C., Burton, N.R. & Lodge, D. (1983) The dissociative anaesthetics, ketamine and phencyclidine, selectively reduce excitation of central mammalian neurones by N-methyl-aspartate. *Br. J. Pharmacol.*, **79**, 565–575.
- Armstrong, D.M. & Rawson, J.A. (1979) Responses of neurones in nucleus interpositus of the cerebellum to cutaneous nerve volleys in the awake cat. *J. Physiol.*, **289**, 403–423.
- Barth, D.S. (2003) Submillisecond synchronization of fast electrical oscillations in neocortex. *J. Neurosci.*, **23**, 2502–2510.
- Brenowitz, S.D. & Regehr, W.G. (2005) Associative short-term synaptic plasticity mediated by endocannabinoids. *Neuron*, **45**, 419–431.
- Buchin, A., Rieubland, S., Häusser, M., Gutkin, B.S. & Roth, A. (2016) Inverse stochastic resonance in cerebellar purkinje cells. *PLoS Comput. Biol.*, **12**, e1005000.
- Chaisanguanthum, K.S., Joshua, M., Medina, J.F., Bialek, W. & Lisberger, S.G. (2014) The neural code for motor control in the cerebellum and oculomotor brainstem. *eNeuro*, **1**, <https://doi.org/10.1523/ENEURO.0004-14.2014>. [Epub ahead of print].
- Chen, X.Y., Wang, Y., Chen, Y., Chen, L. & Wolpaw, J.R. (2016) The inferior olive is essential for long-term maintenance of a simple motor skill. *J. Neurophysiol.*, **116**, 1946–1955.
- Cheron, G., Gall, D., Servais, L., Dan, B., Maex, R. & Schiffmann, S.N. (2004) Inactivation of calcium-binding protein genes induces 160 Hz oscillations in the cerebellar cortex of alert mice. *J. Neurosci.*, **24**, 434–441.
- Cheron, G., Sausbier, M., Sausbier, U., Neuhuber, W., Ruth, P., Dan, B. & Servais, L. (2009) BK channels control cerebellar Purkinje and Golgi cell rhythmicity in vivo. *PLoS ONE*, **4**, e7991.
- Cheron, G., Prigogine, C., Cheron, J., Márquez-Ruiz, J., Traub, R.D. & Dan, B. (2014) Emergence of a 600-Hz buzz UP state Purkinje cell firing in alert mice. *Neuroscience*, **263**, 15–26.
- Courtemanche, R. & Lamarre, Y. (2005) Local field potential oscillations in primate cerebellar cortex: synchronization with cerebral cortex during active and passive expectancy. *J. Neurophysiol.*, **93**, 2039–2052.
- Courtemanche, R., Pellerin, J.-P. & Lamarre, Y. (2002) Local field potential oscillations in primate cerebellar cortex: modulation during active and passive expectancy. *J. Neurophysiol.*, **88**, 771–782.
- Courtemanche, R., Robinson, J.C. & Aponte, D.I. (2013) Linking oscillations in cerebellar circuits. *Front. Neural Circuit.*, **7**, 125.
- Curio, G., Mackert, B.M., Burghoff, M., Koetitz, R., Abraham-Fuchs, K. & Härer, W. (1994) Localization of evoked neuromagnetic 600 Hz activity in the cerebral somatosensory system. *Electroen. Clin. Neurophysiol.*, **91**, 483–487.
- D'Angelo, E., Koekkoek, S.K.E., Lombardo, P., Solinas, S., Ros, E., Garrido, J., Schonewille, M. & De Zeeuw, C.I. (2009) Timing in the cerebellum: oscillations and resonance in the granular layer. *Neuroscience*, **162**, 805–815.
- De Gruijl, J.R., Hoogland, T.M. & De Zeeuw, C.I. (2014) Behavioral correlates of complex spike synchrony in cerebellar microzones. *J. Neurosci.*, **34**, 8937–8947.
- De Zeeuw, C.I. & Berrebi, A.S. (1995) Postsynaptic targets of Purkinje cell terminals in the cerebellar and vestibular nuclei of the rat. *Eur. J. Neurosci.*, **7**, 2322–2333.
- De Zeeuw, C.I., Van Alphen, A.M., Hawkins, R.K. & Ruijgrok, T.J. (1997) Climbing fibre collaterals contact neurons in the cerebellar nuclei that provide a GABAergic feedback to the inferior olive. *Neuroscience*, **80**, 981–986.
- Dugué, G.P., Brunel, N., Hakim, V., Schwartz, E., Chat, M., Lévesque, M., Courtemanche, R., Léna, C. *et al.* (2009) Electrical coupling mediates tunable low-frequency oscillations and resonance in the cerebellar Golgi cell network. *Neuron*, **61**, 126–139.
- Eccles, J.C., Llinás, R. & Sasaki, K. (1966) The excitatory synaptic action of climbing fibres on the Purkinje cells of the cerebellum. *J. Physiol.*, **182**, 268–296.

- English, D.F., Peyrache, A., Stark, E., Roux, L., Vallentin, D., Long, M.A. & Buzsáki, G. (2014) Excitation and inhibition compete to control spiking during hippocampal ripples: intracellular study in behaving mice. *J. Neurosci.*, **34**, 16509–16517.
- Gilbert, P.F. & Thach, W.T. (1977) Purkinje cell activity during motor learning. *Brain Res.*, **128**, 309–328.
- Groth, J.D. & Sahin, M. (2015) High frequency synchrony in the cerebellar cortex during goal directed movements. *Front. Syst. Neurosci.*, **9**, 98.
- Gruart, A. & Delgado-García, J.M. (1994) Discharge of identified deep cerebellar nuclei neurons related to eye blinks in the alert cat. *Neuroscience*, **61**, 665–681.
- Gruart, A., Blázquez, P., Pastor, A.M. & Delgado-García, J.M. (1994) Very short-term potentiation of climbing fiber effects on deep cerebellar nuclei neurons by conditioning stimulation of mossy fiber afferents. *Exp. Brain Res.*, **101**, 173–177.
- Hansel, C., Linden, D.J. & D'Angelo, E. (2001) Beyond parallel fiber LTD: the diversity of synaptic and non-synaptic plasticity in the cerebellum. *Nat. Neurosci.*, **4**, 467–475.
- Heck, D.H., De Zeeuw, C.I., Jaeger, D., Khodakhah, K. & Person, A.L. (2013) The neuronal code(s) of the cerebellum. *J. Neurosci.*, **33**, 17603–17609.
- Hendelman, W.J. & Marshall, K.C. (1980) Axonal projection patterns visualized with horseradish peroxidase in organized cultures of cerebellum. *Neuroscience*, **5**, 1833–1846.
- Hoebeek, F.E., Witter, L., Ruigrok, T.J.H. & De Zeeuw, C.I. (2010) Differential olivo-cerebellar cortical control of rebound activity in the cerebellar nuclei. *Proc. Natl. Acad. Sci. USA*, **107**, 8410–8415.
- Houser, C.R., Barber, R.P. & Vaughn, J.E. (1984) Immunocytochemical localization of glutamic acid decarboxylase in the dorsal lateral vestibular nucleus: evidence for an intrinsic and extrinsic GABAergic innervation. *Neurosci. Lett.*, **47**, 213–220.
- Husson, Z., Rousseau, C.V., Broll, I., Zeilhofer, H.U. & Dieudonné, S. (2014) Differential GABAergic and glycinergic inputs of inhibitory interneurons and Purkinje cells to principal cells of the cerebellar nuclei. *J. Neurosci.*, **34**, 9418–9431.
- Ito, M. (2001) Cerebellar long-term depression: characterization, signal transduction, and functional roles. *Physiol. Rev.*, **81**, 1143–1195.
- Jirenhed, D.-A., Rasmussen, A., Johansson, F. & Hesslow, G. (2017) Learned response sequences in cerebellar Purkinje cells. *Proc. Natl. Acad. Sci. USA*, **114**, 6127–6132.
- Jones, M.S. & Barth, D.S. (1999) Spatiotemporal organization of fast (>200 Hz) electrical oscillations in rat Vibrissa/Barrel cortex. *J. Neurophysiol.*, **82**, 1599–1609.
- Jones, M.S. & Barth, D.S. (2002) Effects of bicuculline methiodide on fast (>200 Hz) electrical oscillations in rat somatosensory cortex. *J. Neurophysiol.*, **88**, 1016–1025.
- Jones, M.S., MacDonald, K.D., Choi, B., Dudek, F.E. & Barth, D.S. (2000) Intracellular correlates of fast (>200 Hz) electrical oscillations in rat somatosensory cortex. *J. Neurophysiol.*, **84**, 1505–1518.
- Kandel, A. & Buzsáki, G. (1997) Cellular-synaptic generation of sleep spindles, spike-and-wave discharges, and evoked thalamocortical responses in the neocortex of the rat. *J. Neurosci.*, **17**, 6783–6797.
- Lefler, Y., Yarom, Y. & Uusisaari, M.Y. (2014) Cerebellar inhibitory input to the inferior olive decreases electrical coupling and blocks subthreshold oscillations. *Neuron*, **81**, 1389–1400.
- Leznik, E. & Llinás, R. (2005) Role of gap junctions in synchronized neuronal oscillations in the inferior olive. *J. Neurophysiol.*, **94**, 2447–2456.
- Llinás, R.R. (2011) Cerebellar motor learning versus cerebellar motor timing: the climbing fibre story. *J. Physiol.*, **589**, 3423–3432.
- Llinás, R.R. (2013) The olivo-cerebellar system: a key to understanding the functional significance of intrinsic oscillatory brain properties. *Front. Neural Circuits.*, **7**, 96.
- Llinás, R. & Mühlethaler, M. (1988) Electrophysiology of guinea-pig cerebellar nuclear cells in the in vitro brain stem-cerebellar preparation. *J. Physiol.*, **404**, 241–258.
- Llinás, R. & Sugimori, M. (1980a) Electrophysiological properties of in vitro Purkinje cell dendrites in mammalian cerebellar slices. *J. Physiol.*, **305**, 197–213.
- Llinás, R. & Sugimori, M. (1980b) Electrophysiological properties of in vitro Purkinje cell somata in mammalian cerebellar slices. *J. Physiol.*, **305**, 171–195.
- Llinás, R. & Yarom, Y. (1986) Oscillatory properties of guinea-pig inferior olivary neurones and their pharmacological modulation: an in vitro study. *J. Physiol.*, **376**, 163–182.
- Llinás, R., Baker, R. & Sotelo, C. (1974) Electrotonic coupling between neurons in cat inferior olive. *J. Neurophysiol.*, **37**, 560–571.
- Long, M.A., Deans, M.R., Paul, D.L. & Connors, B.W. (2002) Rhythmicity without synchrony in the electrically uncoupled inferior olive. *J. Neurosci.*, **22**, 10898–10905.
- Lu, H., Yang, B. & Jaeger, D. (2016) Cerebellar nuclei neurons show only small excitatory responses to optogenetic olivary stimulation in transgenic mice: in vivo and in vitro studies. *Front. Neural Circuits.*, **10**, 21.
- Márquez-Ruiz, J. & Cheron, G. (2012) Sensory stimulation-dependent plasticity in the cerebellar cortex of alert mice. *PLoS ONE*, **7**, e36184.
- Masoli, S., Solinas, S. & D'Angelo, E. (2015) Action potential processing in a detailed Purkinje cell model reveals a critical role for axonal compartmentalization. *Front. Cell. Neurosci.*, **9**, 47.
- Mathy, A., Ho, S.S.N., Davie, J.T., Duguid, I.C., Clark, B.A. & Häusser, M. (2009) Encoding of oscillations by axonal bursts in inferior olive neurons. *Neuron*, **62**, 388–399.
- Mathy, A., Clark, B.A. & Häusser, M. (2014) Synaptically induced long-term modulation of electrical coupling in the inferior olive. *Neuron*, **81**, 1290–1296.
- McCrea, R.A., Bishop, G.A. & Kitai, S.T. (1978) Morphological and electrophysiological characteristics of projection neurons in the nucleus interpositus of the cat cerebellum. *J. Comp. Neurol.*, **181**, 397–419.
- Molinari, M., Leggio, M.G. & Thaut, M.H. (2007) The cerebellum and neural networks for rhythmic sensorimotor synchronization in the human brain. *Cerebellum*, **6**, 18–23.
- Najac, M. & Raman, I.M. (2017) Synaptic excitation by climbing fibre collaterals in the cerebellar nuclei of juvenile and adult mice. *J. Physiol.*, **595**, 6703–6718.
- Paxinos, G. & Franklin, K.B.J. (2004). *The Mouse Brain in Stereotaxic Coordinates*. Gulf Professional Publishing, Houston, TX.
- Popa, L.S., Streng, M.L. & Ebner, T.J. (2017) Long-term predictive and feedback encoding of motor signals in the simple spike discharge of Purkinje cells. *eNeuro*, **4**, <https://doi.org/10.1523/ENEURO.0036-17.2017>. [Epub ahead of print].
- Pugh, J.R. & Raman, I.M. (2006) Potentiation of mossy fiber EPSCs in the cerebellar nuclei by NMDA receptor activation followed by postinhibitory rebound current. *Neuron*, **51**, 113–123.
- Raman, I.M., Gustafson, A.E. & Padgett, D. (2000) Ionic currents and spontaneous firing in neurons isolated from the cerebellar nuclei. *J. Neurosci.*, **20**, 9004–9016.
- Raymond, J.L., Lisberger, S.G. & Mauk, M.D. (1996) The cerebellum: a neuronal learning machine? *Science*, **272**, 1126–1131.
- Robinson, J.C., Chapman, C.A. & Courtemanche, R. (2017) Gap junction modulation of low-frequency oscillations in the cerebellar granule cell layer. *Cerebellum*, **16**, 802–811.
- Ruigrok, T.J.H. & Teune, T.M. (2014) Collateralization of cerebellar output to functionally distinct brainstem areas. A retrograde, non-fluorescent tracing study in the rat. *Front. Syst. Neurosci.*, **8**, 23.
- Sastry, B.R., Morishita, W., Yip, S. & Shew, T. (1997) GABA-ergic transmission in deep cerebellar nuclei. *Prog. Neurobiol.*, **53**, 259–271.
- Schweighofer, N., Lang, E.J. & Kawato, M. (2013) Role of the olivo-cerebellar complex in motor learning and control. *Front. Neural Circuits.*, **7**, 94.
- Servais, L., Bearzatto, B., Schwaller, B., Dumont, M., De Saedeleer, C., Dan, B., Barski, J.J., Schiffmann, S.N. *et al.* (2005) Mono- and dual-frequency fast cerebellar oscillation in mice lacking parvalbumin and/or calbindin D-28k. *Eur. J. Neurosci.*, **22**, 861–870.
- Simon, A., Traub, R.D., Vladimirov, N., Jenkins, A., Nicholson, C., Whitaker, R.G., Schofield, I., Clowry, G.J. *et al.* (2014) Gap junction networks can generate both ripple-like and fast ripple-like oscillations. *Eur. J. Neurosci.*, **39**, 46–60.
- Sokolov, A.A., Miall, R.C. & Ivry, R.B. (2017) The cerebellum: adaptive prediction for movement and cognition. *Trends Cogn. Sci.*, **21**, 313–332.
- de Solages, C., Szapiro, G., Brunel, N., Hakim, V., Isope, P., Buisseret, P., Rousseau, C., Barbour, B. *et al.* (2008) High-frequency organization and synchrony of activity in the purkinje cell layer of the cerebellum. *Neuron*, **58**, 775–788.
- Streng, M.L., Popa, L.S. & Ebner, T.J. (2017) Climbing fibers control Purkinje cell representations of behavior. *J. Neurosci.*, **37**, 1997–2009.
- Sultan, F., König, T., Möck, M. & Thier, P. (2002) Quantitative organization of neurotransmitters in the deep cerebellar nuclei of the Lurcher mutant. *J. Comp. Neurol.*, **452**, 311–323.

- Swensen, A.M. & Bean, B.P. (2003) Ionic mechanisms of burst firing in dissociated Purkinje neurons. *J. Neurosci.*, **23**, 9650–9663.
- Thach, W.T. (1968) Discharge of Purkinje and cerebellar nuclear neurons during rapidly alternating arm movements in the monkey. *J. Neurophysiol.*, **31**, 785–797.
- Traub, R.D. & Bibbig, A. (2000) A model of high-frequency ripples in the hippocampus based on synaptic coupling plus axon-axon gap junctions between pyramidal neurons. *J. Neurosci.*, **20**, 2086–2093.
- Traub, R.D., Middleton, S.J., Knöpfel, T. & Whittington, M.A. (2008) Model of very fast (> 75 Hz) network oscillations generated by electrical coupling between the proximal axons of cerebellar Purkinje cells. *Eur. J. Neurosci.*, **28**, 1603–1616.
- Traub, R.D., Cunningham, M.O. & Whittington, M.A. (2011) Chemical synaptic and gap junctional interactions between principal neurons: partners in epileptogenesis. *Neural Netw.*, **24**, 515–525.
- Traub, R.D., Schmitz, D., Maier, N., Whittington, M.A. & Draguhn, A. (2012) Axonal properties determine somatic firing in a model of in vitro CA1 hippocampal sharp wave/ripples and persistent gamma oscillations. *Eur. J. Neurosci.*, **36**, 2650–2660.
- Uusisaari, M. & Knöpfel, T. (2008) GABAergic synaptic communication in the GABAergic and non-GABAergic cells in the deep cerebellar nuclei. *Neuroscience*, **156**, 537–549.
- Uusisaari, M. & Knöpfel, T. (2011) Functional classification of neurons in the mouse lateral cerebellar nuclei. *Cerebellum*, **10**, 637–646.
- Uusisaari, M., Obata, K. & Knöpfel, T. (2007) Morphological and electrophysiological properties of GABAergic and non-GABAergic cells in the deep cerebellar nuclei. *J. Neurophysiol.*, **97**, 901–911.
- Van Der Giessen, R.S., Maxeiner, S., French, P.J., Willecke, K. & De Zeeuw, C.I. (2006) Spatiotemporal distribution of Connexin45 in the olivocerebellar system. *J. Comp. Neurol.*, **495**, 173–184.
- Wassef, M., Simons, J., Tappaz, M.L. & Sotelo, C. (1986) Non-Purkinje cell GABAergic innervation of the deep cerebellar nuclei: a quantitative immunocytochemical study in C57BL and in Purkinje cell degeneration mutant mice. *Brain Res.*, **399**, 125–135.
- Waterstraat, G., Scheuermann, M. & Curio, G. (2016) Non-invasive single-trial detection of variable population spike responses in human somatosensory evoked potentials. *Clin. Neurophysiol.*, **127**, 1872–1878.
- Welsh, J.P., Lang, E.J., Sugihara, I. & Llinás, R. (1995) Dynamic organization of motor control within the olivocerebellar system. *Nature*, **374**, 453–457.
- White, J.J. & Sillitoe, R.V. (2017) Genetic silencing of olivocerebellar synapses causes dystonia-like behaviour in mice. *Nat. Commun.*, **8**, 14912.
- Woodruff-Pak, D.S. (2006) Stereological estimation of Purkinje neuron number in C57BL/6 mice and its relation to associative learning. *Neuroscience*, **141**, 233–243.